

# Search for emission from Gamma Ray Bursts with the ARGO-YBJ detector

Tristano Di Girolamo<sup>1</sup> for the ARGO-YBJ Collaboration

**Abstract**—ARGO-YBJ is a full coverage air shower detector consisting of a 6700  $m^2$  carpet of Resistive Plate Counters, located at Yangbajing (Tibet, P.R.China, 4300  $m$  a.s.l.). Its large field of view ( $\sim 2$   $sr$ ) makes ARGO-YBJ particularly suitable to detect unpredictable and short duration events such as Gamma Ray Bursts. ARGO-YBJ works using two techniques: the Scaler Mode, which reaches the lower energy limit ( $\sim 1$   $GeV$ ) of the detector, and the Shower Mode, with an energy threshold of a few hundreds of  $GeV$ . Here we present the results of the search for emission from Gamma Ray Bursts in coincidence with satellite detections.

## I. INTRODUCTION

Many theoretical models for Gamma Ray Bursts (GRBs) predict a significant emission above 1  $GeV$ . The high energy gamma rays can result from several processes, both leptonic and hadronic, such as inverse Compton scattering by electrons, electron and proton synchrotron emission, and photopion production, each of them included in a wide variety of models with different hypotheses on the production region, giving different features of the emitted signal (see [1] for a review). Once produced, this high energy radiation is absorbed by the Extragalactic Background Light (EBL) before reaching the Earth, nevertheless the measurements in the  $GeV$ - $TeV$  energy range may reveal the spectral cutoff of GRBs, constraining the emission models. No cutoff energy has been detected till now by satellites up to 1  $GeV$ , forcing the search to more energetic regions. Since the gamma ray extinction increases with distance, and most of the observed GRBs occur at large redshifts, it is important to keep the detectable energy under 100  $GeV$ , where the absorption increases rapidly. However the amount of the EBL is not yet well known, and the detection from ground of the blazar 3C279 at  $z=0.536$  with the MAGIC imaging atmospheric Cherenkov telescope at  $E > 80$   $GeV$  [2] re-emphasized the problem of the opacity of the Universe to gamma rays in the sub- $TeV$  energy range [3].

Above 1  $GeV$ , the detection made by EGRET of only 3 GRBs during 7 years of observations [4], with photons up to 18  $GeV$  (emitted from GRB940217 about 90 minutes after the burst start [5]), indicates that their spectra are usually soft. Recently, the LAT instrument on board the Fermi Gamma-ray Space Telescope announced the detection of more than 10 photons above 1  $GeV$  from GRB080916c [6] (unfortunately this event was below the horizon of our detector). At higher energies, hints ( $\sim 3\sigma$ ) of emission detected at ground have

been reported by Milagrito for GRB970417a ( $E > 650$   $GeV$ ) [7], by the GRAND array for GRB971110 ( $E > 10$   $GeV$ ) [8], and by HEGRA AIROBICC for GRB920925c ( $E > 20$   $TeV$ ) [9]. Moreover, the Tibet Air Shower array found an indication of 10  $TeV$  emission in a stacked analysis of 57 bursts [10]. 40 years after their discovery, and more than 10 years after the detection of the first afterglow by BeppoSAX [11], the physical origin of the enigmatic GRBs is still under debate. The scarcity of information generates a confused situation, allowing a great variety of very different models. This puzzling condition is hampered by the few contradictory experimental results. In this situation, and mainly in the  $> 1$   $GeV$  energy region, any result could be of great importance to approach the solution of the GRB mystery. In this paper, the search for emission in the 1  $GeV$ -1  $TeV$  range in coincidence with satellite detections is presented for several GRBs.

## II. THE DETECTOR

The Astrophysical Radiation with Ground-based Observatory at Yangbajing (ARGO-YBJ), located at the Yangbajing Cosmic Ray Laboratory (30.11°N, 90.53°E, atmospheric depth 606  $g/cm^2$ ), was completely installed in spring 2007. It is made by a single layer of Resistive Plate Counters (RPCs), with a full coverage (92% of active surface) of an area of 5600  $m^2$ , surrounded by a sampling guard ring for a total of 6700  $m^2$ . The apparatus has a modular structure, the basic module being a “cluster” (5.7×7.6  $m^2$ ), divided into 12 RPCs (2.8×1.25  $m^2$  each). The RPCs are working at a high voltage 7200 V with a gas mixture made by 15% Argon, 10% Isobutane and 75% Tetrafluoroethane and a resulting efficiency of 95%. In future a 0.5 cm thick lead converter will cover the apparatus. Since the clusters are working independently, physical studies started since the beginning of the installation, with surface and sensitivity increasing with time.

The detector is connected to two independent data acquisition systems, corresponding to operations in “shower mode” and “scaler mode”. In shower mode the arrival time and the location of each particle are recorded using the highest space-time granularity of the detector, the “pad”, with dimension 55.6×61.8  $cm^2$  (10 pads on each RPC). The current threshold is set to 20 fired pads, corresponding to an energy threshold for photons of a few hundreds of  $GeV$  and a trigger rate of  $\sim 3.8$   $kHz$ . In scaler mode the counts of each cluster are obtained adding up the signal coming from its 120 pads. This signal is put in coincidence in a narrow time window (150 ns) and read by four independent scaler channels, measuring the total counting rate of  $\geq 1$ ,  $\geq 2$ ,  $\geq 3$  and  $\geq 4$  pads fired. The

<sup>1</sup>Università di Napoli “Federico II” and INFN, Dipartimento di Scienze Fisiche, Complesso Universitario Monte S. Angelo, Via Cintia, 80126 Napoli, Italy, tristano@na.infn.it

corresponding trigger rates are  $\sim 40$  kHz,  $\sim 2$  kHz,  $\sim 300$  Hz and  $\sim 120$  Hz. This technique does not allow the measurement of the energy and direction of the primary gamma rays, and the field of view is only limited by the atmospheric absorption, but the energy threshold can be pushed down to  $\sim 1$  GeV, overlapping the highest energies investigated by satellite experiments. Moreover, with four measurement channels sensitive to different energies, in case of positive detection valuable information on the high energy spectrum slope and possible cutoff may be obtained. A detailed description of the detector and its performance can be found in [12], [13] and references therein; the single particle technique applied to the ARGO-YBJ experiment, with the determination of effective area, upper limits calculation and expected sensitivity, can be found in [14].

### III. SEARCH FOR EMISSION FROM GRBS

#### A. SEARCH IN SCALER MODE

Data have been collected from November 2004 (corresponding to the Swift satellite launch) to June 2008, with a detector active area increasing from 693 to 6628  $m^2$ . During this period, a total of 58 GRBs was inside the ARGO-YBJ field of view (i.e. with zenith angle  $\theta \leq 45^\circ$ ); for 19 of them the detector and/or data acquisition were not active or not working properly. The remaining 39 events were investigated searching for a significant excess in coincidence with the satellite detection. In order to extract the maximum information from the data, two GRB analyses have been implemented:

- search for a signal from every single GRB;
- search for a signal from the stack of all GRBs.

For both analyses, the first step is the data cleaning and check. For each event, the Poissonian behaviour of the 4 multiplicity channels ( $\geq 1$ ,  $\geq 2$ ,  $\geq 3$ ,  $\geq 4$ ) for all the clusters is checked using the normalized fluctuation function:

$$f = (s - b)/\sigma, \quad \sigma = \sqrt{b + b/20} \quad (1)$$

for a period of  $\pm 12$  h around the GRB trigger time. In this formula, representing the significance of an excess compared to background fluctuations,  $s$  is the number of counts in a time interval of 10 s and  $b$  the number of counts averaged on a time interval of 100 s before and after the signal, with about 400 independent samples per distribution. The time interval of 10 s has been chosen as the longest surely not affected by the systematic effects given by environment and instrument (such as atmospheric pressure and detector temperature variations). The expected distribution of  $f$  is the standard normal function; all the clusters giving a distribution with measured  $\sigma > 1.2$  or with anomalous excesses in the tail  $\sigma > 3$  (i.e.  $> 2\%$ ), in at least one multiplicity channel, are discarded. This guarantees that our data fulfill the requirements on stability and reliability of the detector. The counting rates of the clusters surviving our quality cuts ( $\sim 92\%$ ) are then added up and the normalized fluctuation function

$$f' = (s' - b')/\sigma', \quad \sigma' = \sqrt{b' + b' \frac{\Delta t_{90}}{600}} \quad (2)$$

is used to give the significance of the coincident on-source counts. In this case  $s'$  is the total number of counts in the  $\Delta t_{90}$  time window given by the satellite detector (corresponding to the detection of 90% of the photons) and  $b'$  is the number of counts in a fixed time interval of 300 s before and after the signal, normalized to the  $\Delta t_{90}$  time. Due to the correlation between different clusters (given by the air shower lateral distribution), the true statistical significance of the on-source counts over the background is obtained again in an interval of  $\pm 12$  h around the GRB time. This calculation is made using equation (17) of Li & Ma [15]; a detailed analysis of the correlation effect and detector stability on counting rates can be found in [14]. The analysis can be done for all the multiplicity channels  $\geq 1$ ,  $\geq 2$ ,  $\geq 3$ ,  $\geq 4$  and 1, 2, 3, where the counting rates  $C$  are obtained from the measured counting rates  $C_{\geq}$  using the relation:

$$C = C_{\geq} - C_{\geq+1} \quad (i = 1, 2, 3) \quad (3)$$

As an example, figure 1 shows the  $f'(C_1)$  distribution for a single cluster and for the sum of all the clusters active during GRB060121; even if the single clusters show a Poissonian behaviour, with width  $\sigma \sim 1$ , the correlation effect on the sum of all clusters broadens the  $f'(\sum C_1)$  distribution ( $\sigma > 1$ ).

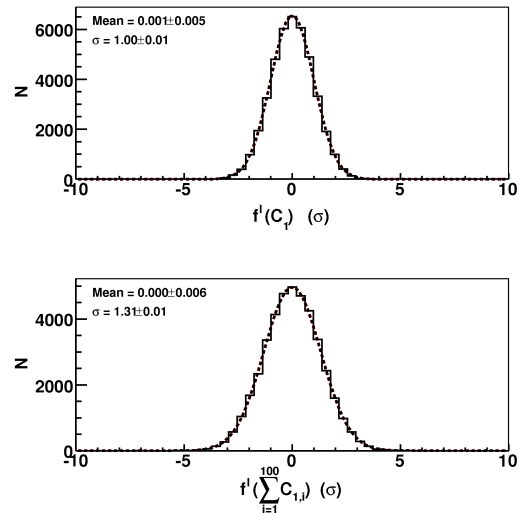


Fig. 1. Experimental distribution of the normalized excesses of signal over background for GRB060121. Top: channel  $C_1$  for a typical cluster compared with a Gaussian fit; bottom: sum of the 100 active clusters.

In the following, all the results are obtained using the counting rate  $C_1$ , since it corresponds to the minimum primary energy in the ARGO-YBJ scaler mode. Figure 2 shows the

distribution of the significances for the whole set of 39 GRBs compared with a standard normal distribution. No significant excess is shown; the mean value is  $0.26\sigma$  and the maximum significance is obtained for GRB051114 ( $3.10\sigma$ ), with a chance probability of 3.8% taking into account the total number of GRBs analyzed.

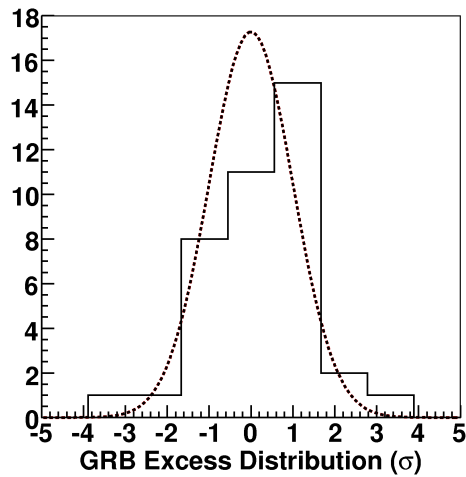


Fig. 2. Distribution of the statistical significances of the 39 GRBs with respect to background fluctuations, compared with a standard normal distribution.

The fluence upper limits are then obtained in the 1-100 GeV energy range adopting a power law spectrum and by considering the maximum number of counts at 99% confidence level (c.l.), following [16]. For this calculation, two different assumptions are used for the power law spectrum: a) extrapolation from the keV-MeV energy region using the spectral index measured by the satellite experiments; b) using a differential spectral index  $\alpha = -2.5$ . Since the mean value of spectral indexes measured by EGRET in the GeV energy region is  $\alpha = -2.0$  [17], we expect that the true upper limits lie between these two values. For those GRBs for which the redshift is known, an exponential cutoff is considered to take into account the effects of the extragalactic absorption and the extinction coefficient is calculated using the values given in [18]. When the redshift is not known, a value of  $z = 1$  is adopted. Figure 3 shows the upper limits obtained extrapolating the keV power law spectra measured by satellites (left) and those obtained assuming a differential index 2.5 (right). Triangles represent GRBs with known redshift.

When using as the GRB spectrum the extrapolation from the keV-MeV region with the spectral index measured by satellite experiments, the upper limit to the cutoff energy can be determined at least for some GRBs. The procedure is the following: the extrapolated fluence is plotted together with our fluence upper limit as a function of the cutoff energy  $E_{\text{cut}}$ .

If the two curves cross in the 2-100 GeV energy range, the intersection gives the upper limit to the cutoff energy. For these GRBs we obtain that, if their spectra should have extended up to  $E_{\text{cut}}$ , it would have produced an increase in counts detectable with a 99% c.l.. Figure 4 shows the resulting cutoff energies.

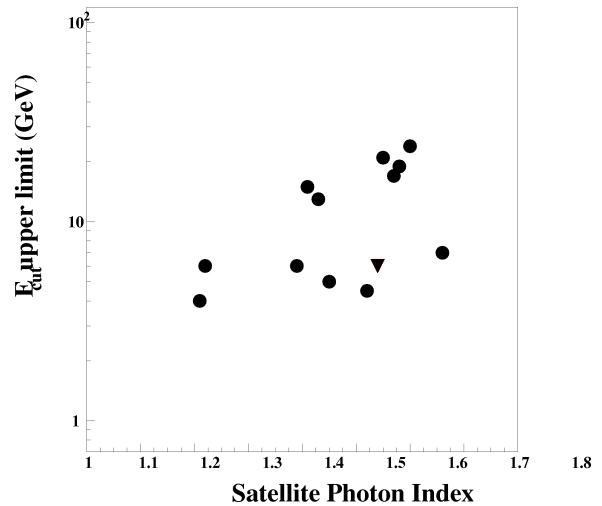


Fig. 4. Upper limits to the cutoff energy. The triangle represents GRB050802, with redshift  $z=1.71$ .

For GRBs with known redshift, a reasonable evaluation of the gamma ray extinction and thus of the upper limits is allowed. Depending on the zenith angle, time duration and spectral index, we obtain fluence upper limits in the 1-100 GeV energy range down to  $4 \times 10^{-6} \text{ erg/cm}^2$ . It is worthwhile to notice that these values greatly depend on the energy range used for the calculation, making meaningless the comparison of upper limits between experiments working in different energy regions. Such a comparison should be done considering the expected number of positive detections under similar hypotheses. For example, the number of GRBs that the MAGIC Telescope can detect is estimated to lie in the range 0.2-0.7 per year [19]. Our estimate, based on similar assumptions (i.e. data from the satellite CGRO) lies between 0.1 and 0.5 per year [14]. The sensitivity of these detectors is thus comparable, even if the fluence upper limits differ for more than 2 decades.

A different analysis is done supposing a common timing feature in all the GRBs. First, the total number of counts in the  $\Delta t$  seconds (with  $\Delta t = 0.5, 1, 2, 5, 10, 20, 50, 100, 200$ ) after  $T_0$  (the low energy trigger time given by the satellite) for all the GRBs has been added up. This is done in order to search for a possible cumulative high energy emission with a fixed duration after  $T_0$ . The resulting significances for the 9 time bins (figure 5) show that there is no evidence of emission for a

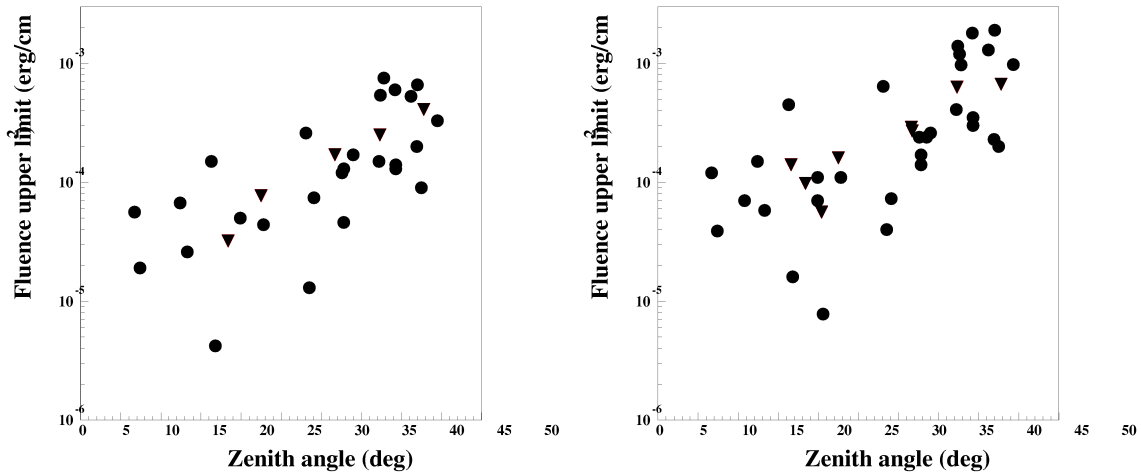


Fig. 3. Fluence upper limits as a function of the zenith angle in the 1-100 GeV range obtained extrapolating the measured keV-MeV spectra (left) or assuming a differential photon index 2.5 (right). For those GRBs with known redshift the upper limits are calculated taking into account the extragalactic absorption (triangles), otherwise  $z = 1$  is assumed (circles).

certain  $\Delta t$ . Since the bins are not independent, the distribution

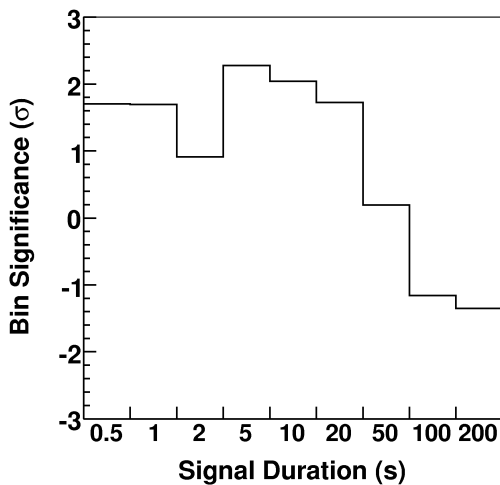


Fig. 5. Significances of GRBs stacked in time for durations between 0.5 and 200 s after the low energy trigger time  $T_0$ .

of the significances of the 9 time bins is compared with random distributions obtained for starting times different from  $T_0$  in a time window of  $\pm 12$  h around the true GRB trigger time. The resulting overall significance of the GRBs stacked in time with respect to random fluctuations is  $0.27 \sigma$ .

A second search is done to test the hypothesis that the high energy emission occurs at a certain phase of the low energy burst, independently of the GRB duration. For this study, all the 33 GRBs with  $\Delta T_{90} \geq 5$  s (i.e. belonging to the “long GRB” population) have been added up in phase scaling their duration. This choice has been done for both physical and technical reasons, adding up the counts for GRBs of the same class and long enough to allow a phase plot with 10 bins given our time resolution of 0.5 s. Figure 6 shows the resulting significances for the 10 phase bins; no evidence of emission at a certain phase is obtained, and the overall significance of the GRBs stacked in phase (obtained adding up all the bins) with respect to background fluctuations is  $0.36 \sigma$ .

This search, for both GRBs stacked in time and in phase, could give a significant signal even if the emission of each GRB is lower than the sensitivity of our detector. In this case, less information could be given with respect to the single GRB coincident detection, but we must consider that with the stacked analysis we increase our sensitivity by increasing the number of GRBs, while for the single GRB search we decrease our sensitivity because of the increasing number of trials.

#### B. SEARCH IN SHOWER MODE

Data collected from July 2006 to July 2008 have been analyzed around the trigger time of 20 GRBs detected by satellites inside the ARGO-YBJ field of view. No significant excess was found for any of them. 99% c.l. upper limits to the fluence were determined assuming a power law spectrum with differential index  $\alpha = -2.0$ , considering absorption by the EBL when the redshift was available. The lowest values are  $\approx 10^{-5} \text{ erg/cm}^2$  in the 10 GeV–1 TeV range. More details

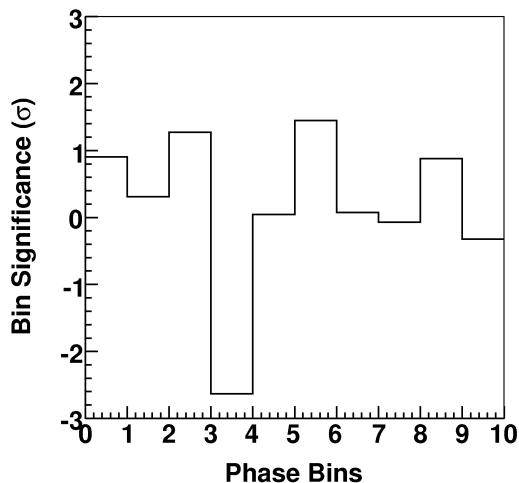


Fig. 6. Significances of GRBs with duration  $\Delta T_{90} \geq 5$  s stacked in 10 phase bins.

about this analysis, together with a discussion of its results, are in [20].

#### IV. CONCLUSIONS

Combining operations in scaler and shower modes, the ARGO-YBJ experiment allows the study of GRBs in the whole 1 GeV–1 TeV range. In the search for high energy emission in coincidence with GRBs detected by satellites, no significant excess was found for any event. The search for a cumulative signal in scaler mode, stacking GRBs both in time and phase, has shown no deviation from the statistical expectations. The derived fluence upper limits reach values as low as  $\approx 10^{-5} \text{ erg/cm}^2$  both in the 1-100 GeV range, using data collected in scaler mode, and in the 10 GeV-1 TeV region, with shower mode data. Since upper limits to the cutoff energy can be set for several GRBs between 2 and 100 GeV, we can conclude that the simple extrapolation of the power law spectra measured at low energies is not always possible [21].

#### REFERENCES

- [1] P. Mészáros, Rep. Prog. Phys. 69, 2259 (2006)
- [2] J. Albert et al., Science 320, 1752 (2008)
- [3] F.W. Stecker & S.T. Scully, arXiv:0807.4880 (2008), submitted to The Astrophysical Journal Letters.
- [4] J.R. Catelli, B.L.Dingus and E.J.Schneid, *Gamma Ray Bursts*, edited by C.A. Meegan, AIP Conf. Proc. 428, 309 (1997)
- [5] K. Hurley, Nature 372, 652 (1994)
- [6] H. Tajima et al., GCN Circular 8246 (2008)
- [7] R. Atkins et al., The Astrophysical Journal 533, L119 (2000)
- [8] J. Poirier et al., Physical Review D 67, 042001 (2003)
- [9] L. Padilla et al., Astronomy & Astrophysics 337, 43 (1998)
- [10] M. Amenomori et al., Astronomy & Astrophysics 311, 919 (1996)
- [11] E. Costa et al., Nature 387, 783 (1997)
- [12] G. Aielli et al., Nuclear Instruments and Methods A562, 92 (2006)
- [13] G. Di Sciascio et al., arXiv:0811.0997 (2008), Proceedings of the Vulcano Workshop 2008, in press

- [14] G. Aielli et al., Astroparticle Physics 30, 85 (2008)
- [15] T. Li and Y. Ma, The Astrophysical Journal 272, 317 (1983)
- [16] O. Helene, Nuclear Instruments and Methods 212, 319 (1982)
- [17] B.L. Dingus, J.R. Catelli and E.J. Schneid, Proc. 25th ICRC, vol. 3, p.29 (1997)
- [18] T.M. Kneiske, T. Bretz, K. Mannheim, D.H. Hatmann, Astronomy and Astrophysics 413, 807 (2004)
- [19] J. Albert et al., The Astrophysical Journal 667, 358 (2007)
- [20] S.Z. Chen et al., Proceedings of the Nanjing GRB Conference, June 2008.
- [21] D. Band et al., The Astrophysical Journal 413, 281 (1993)